Hindawi
Journal of Nanomaterials
Volume 2022, Article ID 2892738, 9 pages
https://doi.org/10.1155/2022/2892738

Research Article

Artificial Intelligence Investigation on (Al-Si-Fe) Alloy Reinforced with Nanoceramic Particles by RSM

S. K. Rajesh Kanna,[1] G. Naveen Sundar,[2] R. Ganesan,[3] Naresh Mallireddy,[4] Hitesh Shingadia,[5] Harishchander Anandaram,[6] Melvin Victor De Poures,[7] and Prabhu Paramasivam[8]

[1]*Department of Mechanical Engineering, Rajalakshmi Institute of Technology, Chennai, India*
[2]*Department of Computer Science and Engineering, Karunya Institute of Technology and Sciences, Coimbatore, India*
[3]*Institute of Civil Engineering, Saveetha School of Engineering, Saveetha Institute of Medical and Technical Sciences, Chennai, India*
[4]*Department of Computer Science and Engineering, Aditya College of Engineering, Surampalem, Andhra Pradesh, India*
[5]*Department of Zoology, SVKM's Mithibai College of Arts, Chauhan Institute of Science and Amrutben Jivanlal College of Commerce and Economics (Autonomous), Maharashtra, India*
[6]*Centre for Computational Engineering and Networking, Amrita School of Engineering, Coimbatore, Amrita Vishwa Vidyapeetham, India*
[7]*Department of Thermal Engineering, Saveetha School of Engineering, Saveetha Institute of Medical and Technical Sciences, Chennai, India*
[8]*Department of Mechanical Engineering, College of Engineering and Technology, Mettu University, Ethiopia 318*

Correspondence should be addressed to Prabhu Paramasivam; prabhuparamasivam21@gmail.com

Received 16 July 2022; Revised 12 September 2022; Accepted 21 September 2022; Published 6 October 2022

Academic Editor: S.K. Khadheer Pasha

Copyright © 2022 S. K. Rajesh Kanna et al. This is an open access article distributed under the Creative Commons Attribution License, which permits unrestricted use, distribution, and reproduction in any medium, provided the original work is properly cited.

Al 4043 alloy is extensively used as a filler material for welding aluminum alloys, especially when welding alloys from the Al 6000 series. It is utilized in aerospace and automotive structural components. For longer life in automotive applications, the wear resistance of Al 4043 alloy must be improved. According to research, tungsten carbide has good wear resistance. In this research, Al 4043 alloy is reinforced with varying percentages (1, 3, and 5%) of nano-sized tungsten carbide to increase wear resistance. Taguchi L27 orthogonal array is employed for the wear analysis. The Taguchi signal-to-noise ratio is used to determine the optimal parameters for minimizing wear and coefficient of friction. The regression model and artificial neural network are developed to predict the experimental results. The outcomes of the regression model and artificial neural network are compared to the experimental results to demonstrate both models' efficacy. A confirmation test was carried out for the optimal process parameter. The result shows that the minimized specific wear rate of 0.12 mm^3/Nm, coefficient of friction of 0.01, and frictional force of 1.02 N are achieved at the optimal combination.

1. Introduction

Al 4043 alloy has strong corrosion resistance and is widely utilized as a filler material in welding aluminum, aerospace, and automobile structures [1, 2]. It is mainly used for welding aluminum alloys of the 6000 series [3]. Also, Al 4043 alloy is used in automobile parts like cylinder blocks, cylinder heads, and engine pistons [4]. It is necessary to increase the wear resistance of Al 4043 alloy for a better life. Research illustrates that tungsten carbide reduces the wear when added as an alloying element [5]. Also, the tungsten carbide machining tool shows less resistance to wear in turning operations [6]. Another research shows that increasing the percentage of tungsten carbide reduces the wear of Al 5052 metal matric composite [7]. The hardness is improved, and the coefficient of friction (COF) and wear rate are minimized

Table 1: Experimental values from wear analysis.

S. no	Composition	Load (*N*)	Speed (RPM)	Sliding distance (m)	COF	Sp. wear rate mm^3/Nm	Friction force (*N*)
1	1	14.715	100	25	0.21	2.45	1.2
2	1	14.715	100	25	0.21	2.45	1.2
3	1	14.715	100	25	0.21	2.45	1.2
4	1	29.43	200	55	0.26	0.61	2.6
5	1	29.43	200	55	0.26	0.61	2.6
6	1	29.43	200	55	0.26	0.61	2.6
7	1	44.145	300	90	0.28	0.29	5.3
8	1	44.145	300	90	0.28	0.29	5.3
9	1	44.145	300	90	0.28	0.29	5.3
10	3	14.715	200	90	0.22	0.53	1.98
11	3	14.715	200	90	0.21	0.51	1.5
12	3	14.715	200	90	0.21	0.52	1.5
13	3	29.43	300	25	0.06	0.98	1.5
14	3	29.43	300	25	0.26	0.98	2.6
15	3	29.43	300	25	0.26	0.97	2.6
16	3	44.145	100	55	0.01	1.72	1.98
17	3	44.145	100	55	0.63	1.74	7.43
18	3	44.145	100	55	0.15	1.73	3.2
19	5	14.715	300	55	0.01	0.31	0.5
20	5	14.715	300	55	0.03	0.35	0.8
21	5	14.715	300	55	0.01	0.33	0.8
22	5	29.43	100	90	0.06	0.16	1.1
23	5	29.43	100	90	0.06	0.17	1.1
24	5	29.43	100	90	0.05	0.19	1.3
25	5	44.145	200	25	0.07	0.52	2.1
26	5	44.145	200	25	0.11	0.53	2.3
27	5	44.145	200	25	0.13	0.55	3.32

when the tungsten carbide is added to the titanium alloy matrix [8, 9]. Adding nano-sized particles as an adjuvant decreases agglomeration during material preparation [10]. Hence, in this research, nano-sized tungsten carbide is used as an additive element for improving the wear resistance of Al 4043 alloy.

Taguchi is a robust design of experiments proposed by Genechi Taguchi, which helps us to conduct the experiments methodically with the minimum number of iterations [11]. It gives different combinations of parameters at various factors with optimal runs, which helps the researcher to find the response under various conditions [12, 13]. The Taguchi signal-to-noise ratio is used to determine the optimal process parameter among the experiments for minimizing or maximizing the experimental outcome [14, 15].

The objective of this research is to reduce the wear rate of Al 4043 alloy. The literature review illustrates that adding WC as a reinforcement increases the wear resistance characteristics [16]. Hence, to improve the wear resistance of Al 4043 alloy, different percentages of (1%, 3%, and 5%) nano-sized WC are added to the Al 4043 alloy using a stir casting process. The obtained combinations of metal matrix composite (MMC) are tested in the pin-on-test wear testing apparatus. The experiment uses the L27 Taguchi orthogonal array, and the optimal process parameters are found using signal-to-noise ratio analysis. MINITAB is used for regression analysis to obtain the equation for the response output. Further artificial neural network (ANN) is used to predict the responses for the L27 array. The residuals obtained from the ANN model and the regression analysis are compared with the actual experimental outcome to illustrate the effectiveness of the predicted outcomes.

2. Methodology

2.1. Preparation of Alloy. The Al 4043 alloy is heated in the graphite crucible to a temperature of 900°C. When the alloy reaches the pouring temperature, the stirrer is placed in the crucible, and the stirring begins [17]. Then, the nanoparticle size of tungsten carbide is weighted by 1% added to the crucible. The mixture is stirred for half an hour at 400 rpm at 950°C to get the proper alloy mixture [18]. Then, the alloy is poured into the cylindrical die of 25 mm in diameter and 250 mm in length and solidifies in the atmospheric condition. Then, the same process is repeated to get the Al 4043 with 3% and 5% of tungsten carbide (WC) [19]. The

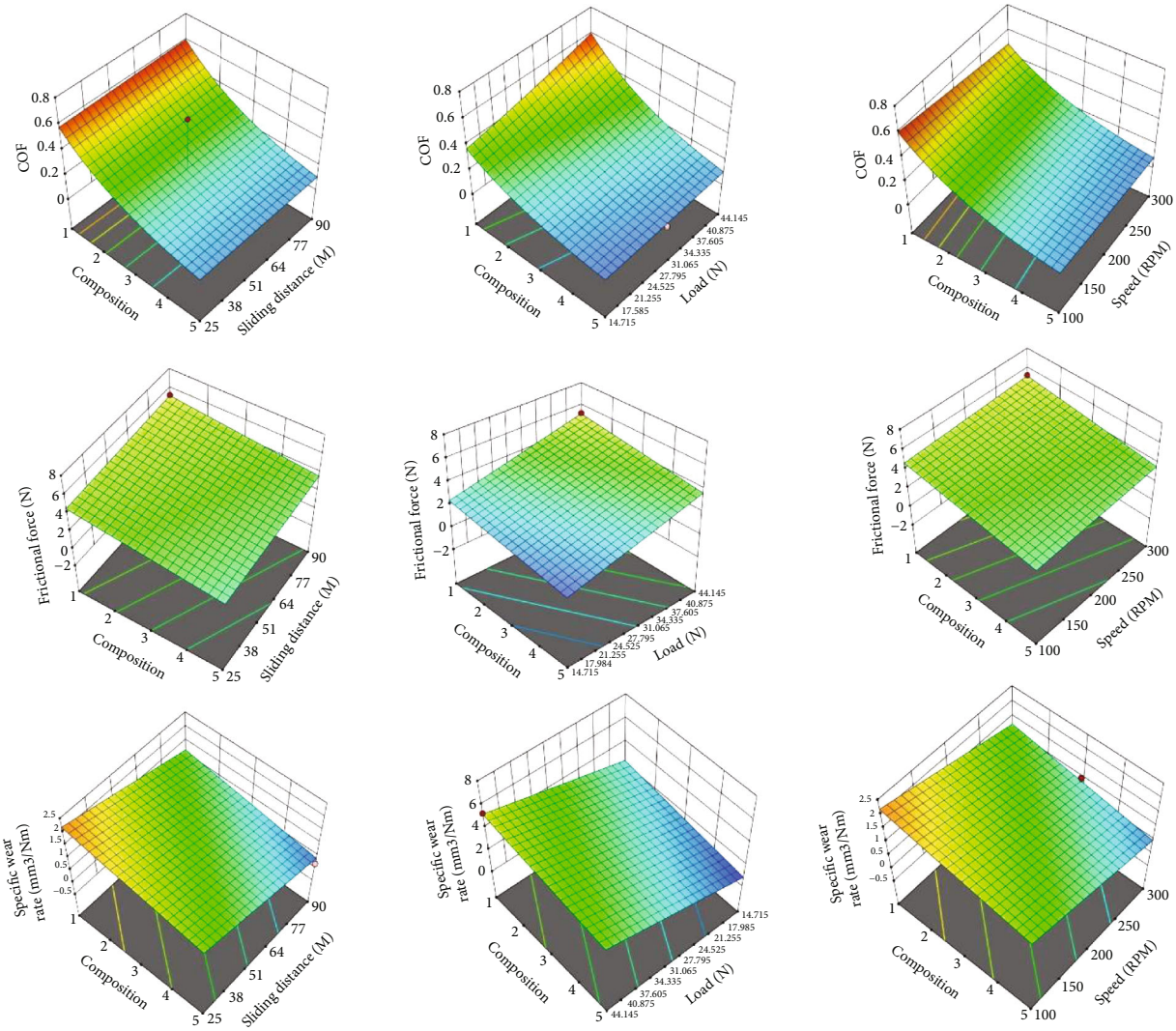

Figure 1: Output response characteristics of processed MMCs by 3D plots.

different compositions of the metal matrix composite (MMC) made for the wear analysis are shown below: (i) Al 4043 of 850 gm and 1% of WC of 8.5 gm; (ii) Al 4043 of 850 gm and 3% of WC of 25.5 gm; and (iii) Al 4043 of 850 gm and 5% of WC of 42.5 gm.

Then, each cylindrical specimen is machined to 6 mm diameter and 15 mm height for the wear analysis [20]. The wear analysis is conducted with EN 24 alloy in the pin on the disc wear testing apparatus. The disc En 24 alloys are polished to make the surface smooth and even throughout. Three different loads are taken for the experiment to analyze the wear of Al 4043 MMC with tungsten carbide; they are 14.715 N, 29.43 N, and 44.145 N.

2.2. Experimental Design. The wear analysis is conducted at room temperature with a relative humidity of 65% at 30 ⊠C. Three different loads are taken for the experiment to analyze the wear of Al 4043 alloy with tungsten carbide; they are 14.715 N, 29.43 N, and 44.145 N. The disc is rotated at three different speeds, 100 N, 200 N, and 300 N, to evaluate the wear of the Al 4043 MMC [21]. The experiment is conducted based on the Taguchi L27 orthogonal array. The result is then optimized using Taguchi signal-to-noise ratio analysis to identify the optimal WC-Al 4043 MMC to minimize wear rate. Regression analysis is used to create a mathematical equation based on the collected results for the chosen input parameter to forecast the outcome for different input parameters. Also, as discussed in the Introduction section, ANN model is used to predict and validate the result obtained from regression equations.

3. Results and Discussion

The experiment is conducted based on L27 Taguchi orthogonal array design, as shown in Table 1. The mass loss (Δm) due to the wear test is calculated by measuring the weight of each pin before and after the experiment. The coefficient of friction (COF) and specific wear rate are calculated using the following equations.

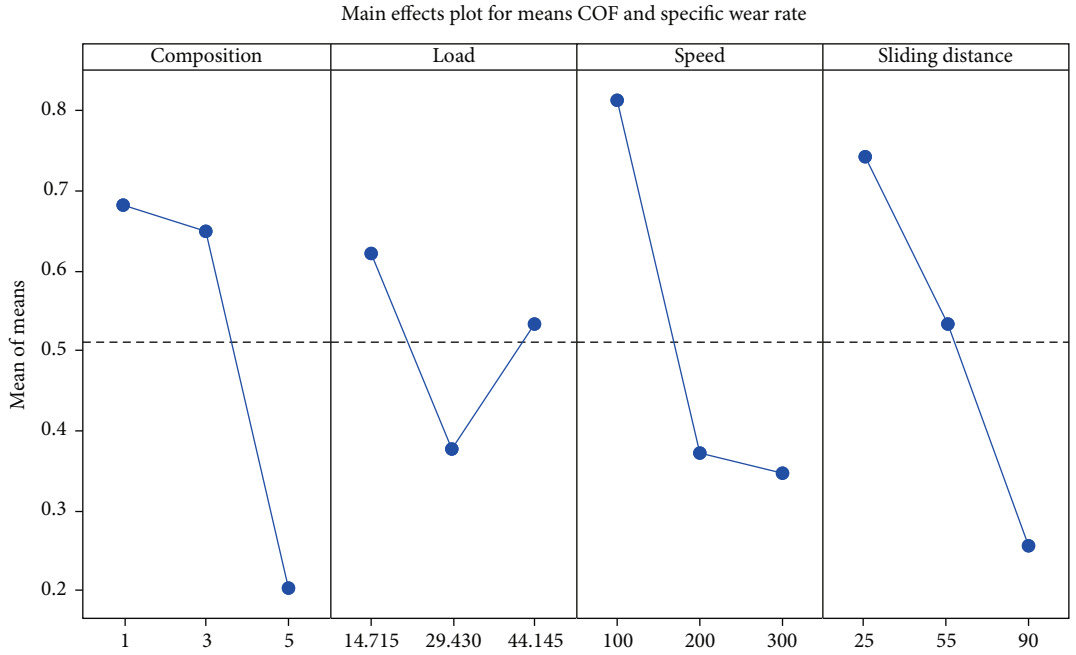

Figure 2: Main effect plot of means for COF and specific wear rate.

Table 2: Experimental and predicted response for optimal condition.

Optimal conditions	Responses	Experimental value	Predicted outcome	Error percentage
Load =29.34 N rotating speed =300 RPM Sliding distance =90 m	COF	0.01	0.014	0.4
	Specific wear rate (mm^3/Nm)	0.12	0.15	0.25
	Frictional force (N)	1.02	0.97	0.04902

$$\text{Co} - \text{efficient of friction} : \mu = \frac{\text{Ff}}{\text{Fn}}, \tag{1}$$

$$\text{Specific wear rate} : \text{Ks} = \frac{\left((\Delta m/\rho \text{LFn})\text{mm}^3\right)}{N - m}, \tag{2}$$

where Δm is the mass loss (g), ρ is the density of the pin material (g/cm^3), L is the sliding distance, Fn denotes load (N), and Ff is the measured frictional force (N) from the experiment.

For each experiment, the En 24disc is completely grinded and polished to remove the wear track, and the flatness is ensured by spirit level measured at different locations. The COF and specific wear rate from the experimental result are calculated based on Equations (1) and (2), and the result is shown in Table 1.

Figure 1 illustrates the 3D surface plot between the input and the responses. From Figure 1, it is seen that COF reduces by increasing the composition of WC. The minimum COF is achieved at the 5% WC with Al 4043. COF is decreased even though the rotational speed of the EN 24 disc is increased. And this proves that the frictional force is reduced with the increase of WC [22]. Also, at a maximum load of 44.145 N, the COF is reduced to the rise in the percentage of WC.

Similarly, the specific wear rate is reduced with the increase in the percentage of WC with Al 4043. The wear rate is minimum at 5% WC with all different loading conditions (14.715 N, 29.43 N, 44.145 N). Hence, it is concluded from Figure 1 that with the increase in the percentage of nano-sized WC with Al 4043 alloy, the COF, frictional force, and specific wear rate are reduced [23].

Taguchi signal-to-noise ratio is used to determine the optimal parameter for minimizing the specific wear rate and coefficient of friction. The analysis is carried out using MINITAB software [24]. From the software, smaller the better characteristics are used to find the optimal process parameter, and the equation for smaller the better characteristics is shown in [25]

$$\text{S/N ratio smaller the better characteristics} = -10 * \log 10\left[\frac{£y^2}{n}\right]\sum. \tag{3}$$

Figure 2 depicts the signal-to-noise ratio result for the optimal parameter for minimizing the COF and specific wear rate. According to the main effect plot for means in Figure 2, the best outcome was reached in 5% WC with Al 4043 alloy, 29.34 N of load, rotating speed of 300 rpm, and sliding distance of 90 m [26]. The experiment is again

Table 3: Experimental values compared with predicted values from regression equations.

Taguchi L27 Array	Experimental values			Values predicted from regression equations			Residuals		
	COF	Sp. wear rate mm^3/Nm	Friction force (N)	COF	Sp. wear rate mm^3/Nm	Friction force (N)	COF	Sp. wear rate	Friction force
1	0.21	2.45	1.2	0.23	2.29	1.14	-0.02	0.15	0.05
2	0.21	2.45	1.2	0.23	2.2	1.14	-0.02	0.150	0.05
3	0.21	2.45	1.2	0.23	2.29	1.14	-0.028	0.150	0.05
4	0.26	0.61	2.6	0.27	1.25	3.16	-0.012	-0.64	-0.56
5	0.26	0.61	2.6	0.27	1.25	3.16	-0.012	-0.64	-0.56
6	0.26	0.61	2.6	0.27	1.25	3.16	-0.012	-0.64	-0.56
7	0.28	0.29	5.3	0.30	0.13	5.23	-0.028	0.151	0.06
8	0.28	0.29	5.3	0.30	0.13	5.23	-0.028	0.151	0.06
9	0.28	0.29	5.3	0.30	0.13	5.2	-0.028	0.15	0.06
10	0.22	0.53	1.98	0.15	0.46	1.34	0.069	0.06	0.63
11	0.21	0.51	1.5	0.15	0.46080	1.34	0.059	0.049	0.15
12	0.21	0.52	1.5	0.15	0.46	1.34	0.059	0.05	0.15
13	0.06	0.98	1.5	0.16	0.87	2.34	-0.10	0.10	-0.84
14	0.26	0.98	2.6	0.16	0.87	2.34	0.096	0.10	0.25
15	0.26	0.97	2.6	0.16	0.87	2.34	0.096	0.099	0.25
16	0.01	1.72	1.98	0.21	1.2	3.5	-0.20	0.51	-1.54
17	0.63	1.74	7.43	0.21	1.20	3.52	0.411	0.53	3.9
18	0.15	1.73	3.2	0.21	1.20	3.52	-0.06	0.523	-0.32
19	0.01	0.31	0.5	0.04	0.15	0.46	-0.030	0.159	0.03
20	0.03	0.35	0.8	0.04	0.15	0.46	-0.010	0.199	0.33
21	0.01	0.33	0.8	0.04	0.15	0.46	-0.030	0.17	0.33
22	0.06	0.16	1.1	0.09	0.41	1.70	-0.035	-0.250	-0.60
23	0.06	0.17	1.1	0.09	0.41	1.70	-0.035	-0.240	-0.60
24	0.05	0.19	1.3	0.09	0.41	1.70	-0.045	-0.220	-0.40
25	0.07	0.52	2.1	0.10	0.82	2.70	-0.039	-0.30	-0.60
26	0.11	0.53	2.3	0.10	0.82	2.70	0.00063	-0.290	-0.40
27	0.13	0.55	3.32	0.10	0.82	2.70	0.020	-0.27	0.61

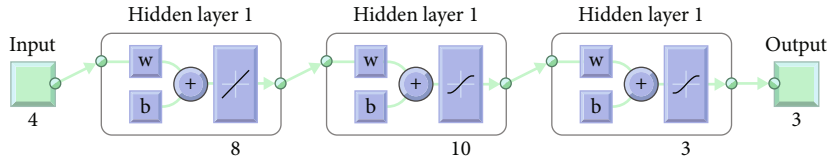

Figure 3: ANN model for the experimental outcome.

conducted for this optimal condition to check the effect of COF and specific wear rate. The obtained result for the optimal parameter is shown in Table 2 [27].

The regression analysis is conducted using the MINITAB software to determine the equations for the COF (4), specific wear rate (5), and frictional force (6) as shown in

$$\text{COF} = 0.2528 * \alpha + 0.00234 * \beta - 0.000067 * \gamma + 0.000219 * \lambda, \quad (4)$$

$$\text{Specific Wear Rate} = 3.458 - 0.1928 * \alpha - 0.00846 * \beta - 0.004594 * \gamma - 0.01529 * \lambda, \quad (5)$$

$$\text{Frictional Force} = -0.422 - 0.388 * \alpha + 0.0965 * \beta + 0.00277 * \gamma + 0.01074 * \lambda, \quad (6)$$

where α denotes composition, β denotes load, and γ and λ represent speed and sliding distance. The experiment is carried out for the optimal condition, and the output

Table 4: Experimental values compared with the ANN predicted values.

Taguchi L27 Array	Experimental values			Values predicted from regression equations			Residuals		
	COF	Sp. wear rate mm^3/Nm	Friction force (N)	COF	Sp. wear rate mm^3/Nm	Friction force (N)	COF	Sp. wear rate	Friction force
1	0.21	2.45	1.2	0.20	2.4477	1.1985	0.00064	0.0023	0.0015
2	0.21	2.45	1.2	0.20936	2.4477	1.1985	0.00064	0.0023	0.0015
3	0.21	2.45	1.2	0.20936	2.4477	1.1985	0.00064	0.0023	0.0015
4	0.26	0.61	2.6	0.24738	0.59965	2.6066	0.01262	0.01035	-0.0066
5	0.26	0.61	2.6	0.24738	0.59965	2.6066	0.01262	0.01035	-0.0066
6	0.26	0.61	2.6	0.24738	0.59965	2.6066	0.01262	0.01035	-0.0066
7	0.28	0.29	5.3	0.31241	0.32606	5.2961	-0.03241	-0.03606	0.0039
8	0.28	0.29	5.3	0.31241	0.32606	5.2961	-0.03241	-0.03606	0.0039
9	0.28	0.29	5.3	0.31241	0.32606	5.2961	-0.03241	-0.03606	0.0039
10	0.22	0.53	1.98	0.20074	0.93881	1.6674	0.01926	-0.40881	0.3126
11	0.21	0.51	1.5	0.20074	0.93881	1.6674	0.00926	-0.42881	-0.1674
12	0.21	0.52	1.5	0.20074	0.93881	1.6674	0.00926	-0.41881	-0.1674
13	0.06	0.98	1.5	0.18243	0.99874	2.093	-0.12243	-0.01874	-0.593
14	0.26	0.98	2.6	0.18243	0.99874	2.093	0.07757	-0.01874	0.507
15	0.26	0.97	2.6	0.18243	0.99874	2.093	0.07757	-0.02874	0.507
16	0.01	1.72	1.98	0.3399	1.5002	5.2805	-0.3299	0.2198	-3.3005
17	0.63	1.74	7.43	0.3399	1.5002	5.2805	0.2901	0.2398	2.1495
18	0.15	1.73	3.2	0.3399	1.5002	5.2805	-0.1899	0.2298	-2.0805
19	0.01	0.31	0.5	0.024652	0.32558	0.66947	-0.01465	-0.01558	-0.16947
20	0.03	0.35	0.8	0.024652	0.32558	0.66947	0.005348	0.02442	0.13053
21	0.01	0.33	0.8	0.024652	0.32558	0.66947	-0.01465	0.00442	0.13053
22	0.06	0.16	1.1	0.07686	0.23104	1.1952	-0.01686	-0.07104	-0.0952
23	0.06	0.17	1.1	0.07686	0.23104	1.1952	-0.01686	-0.06104	-0.0952
24	0.05	0.19	1.3	0.07686	0.23104	1.1952	-0.02686	-0.04104	0.1048
25	0.07	0.52	2.1	0.1194	0.54476	2.2662	-0.0494	-0.02476	-0.1662
26	0.11	0.53	2.3	0.1194	0.54476	2.2662	-0.0094	-0.01476	0.0338
27	0.13	0.55	3.32	0.1194	0.54476	2.2662	0.0106	0.00524	1.0538

responses are illustrated in Table 2. The values of COF, specific wear rate, and frictional force are reduced for the optimal condition [28]. The predicted outcomes using the regression equation for the optimal condition are shown in Table 2. The error percentage shows that the predicted outcomes align with the experimental outcomes [29].

Table 3 shows the residuals computed from the input parameters using Equations (4), (5), and (6). The residual represents the discrepancy between the experimental and predicted values [30]. The residuals are minimal, indicating that the regression equation is accurate. These equations can predict the response outcome for the different input values [31].

As discussed in the introduction, the ANN model is used to predict the specific wear rate, COF, and sliding distance for the L27 array. Figure 3 depicts an ANN model with several layers linked. The working of ANN is identical to the human brain, which receives the input nodes (L27 array) and predicts the response based on weighing the experimental output [18, 20]. These predicted network values (response) are compared to the actual experimental values, and the error is feedback as an input. Then, the bias and feedback are modified, and the networks are redesigned to nullify the error difference to the acceptable value. This iteration process continues until we get the predicted values with acceptable error. Table 4 signifies the predicted values from the neural network and their residuals, and Figure 4 represents the regression plots of training, testing, and validation of the ANN model. Table 4 also compares the experimental results to the ANN predicted values, revealing that the ANNN model predicts the responses with high accuracy.

The present work illustrates the wear behavior of Al 4043 with various percentages of nano-sized WC (1%, 3%, and 5%). From the experiment, the wear rate is reduced with the increase in the percentage of WC. Also, the frictional force is reduced at 5% of WC. Although there is an increase in load and sliding distance, the load and rotational speed are the most significant parameters for increasing the wear rate and COF. The wear due to load and rotational speed is reduced at 5% of WC with Al 4043. The regression equations and ANN model are used to predict the values of the experimental response. The residuals of the regression

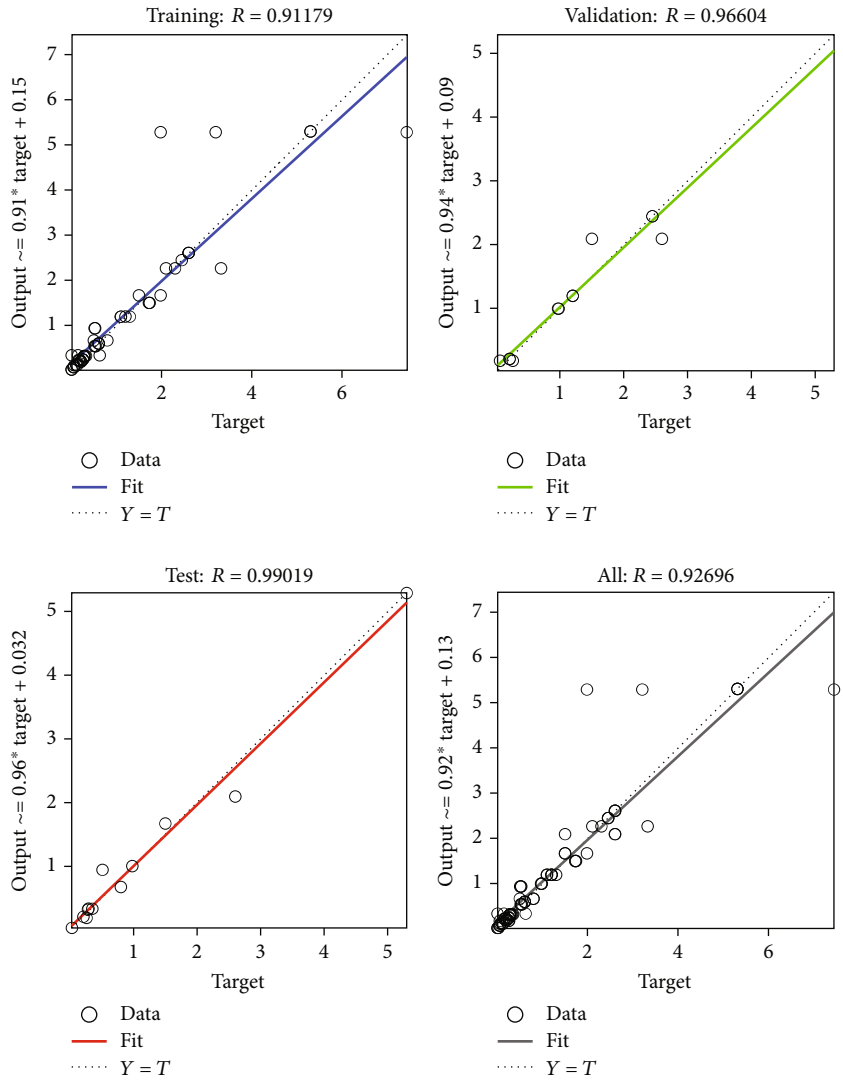

Figure 4: ANN regression graph of training, testing, validation, and complete of all.

equation and ANN model show the accuracy of the predicted values.

4. Conclusion

The present work studies the wear behavior of Al 4043 alloy with the varying percentage of nano-sized WC (1%, 3%, and 5%) which has the following conclusion:

(i) The increase in the percentage of nano-sized WC (5%) reduces the frictional force and specific wear rate of Al 4043

(ii) The optimal parameter for the minimum specific wear rate, COF, is achieved at the following combinations: composition =5% WC with Al 4043, load =29.34 N, rotating speed =300 RPM, and sliding distance =90 m. The experiment was conducted for the optimal combination, and the obtained responses achieved better results than the experimental outcome

(iii) The regression equation developed for the experimental outcome predicts the responses with minimum residuals

(iv) ANN model also well predicted the experimental outcome with minimum residuals

(v) From the experiment, it is concluded that among all the combinations of WC, 5% nano-sized WC reduces the wear rate and COF of Al 4043 alloy

Data Availability

The data used to support the findings of this study are included within the article. Should further data or information be required, these are available from the corresponding author upon request.

Conflicts of Interest

The authors declare that there are no conflicts of interest regarding the publication of this paper.

References

[1] G. Saad, S. A. Fayek, A. Fawzy, H. N. Soliman, and G. Mohammed, "Deformation characteristics of Al-4043 alloy," *Materials Science and Engineering A*, vol. 527, no. 4–5, pp. 904–910, 2010.

[2] Q. Miao, D. Wu, D. Chai et al., "Comparative study of microstructure evaluation and mechanical properties of 4043 aluminum alloy fabricated by wire-based additive manufacturing," *Desmos*, vol. 186, p. 108205, 2020.

[3] M. M. Tawfik, M. M. Nemat-Alla, and M. M. Dewidar, "Enhancing the properties of aluminum alloys fabricated using wire + arc additive manufacturing technique - A review," *Journal of Materials Research and Technology*, vol. 13, pp. 754–768, 2021.

[4] V. Sivaprakash, L. Natrayan, R. Suryanarayanan, R. Narayanan, and P. Paramasivam, "Electrochemical anodic synthesis and analysis of TiO_2 nanotubes for biomedical applications," *Journal of Nanomaterials*, vol. 2021, Article ID 9236530, 10 pages, 2021.

[5] Z. Xu, Z. Zhao, D. Han, Q. Chen, and Z. Li, "Effects of Si content and aging temperature on wear resistance of surfacing layers welded with 4043 aluminum welding wires," *Materials Engineering*, vol. 45, no. 1, pp. 71–74, 2016.

[6] T. Panneerselvam, T. K. Kandavel, and P. Kishore, "Experimental investigation on cutting tool performance of newly synthesized P/M alloy steel under turning operation," *Journal of Engineering Science*, vol. 44, no. 6, pp. 5801–5809, 2019.

[7] P. Anand, D. Rajesh, N. Lenin, V. Balaji, V. K. Bupesh Raja, and K. Palanikumar, "Enhancement of mechanical characterisation of aluminum alloy with tungsten carbide metal matrix composite by particulate reinforcements," *Materials Today: Proceedings*, vol. 46, 2021.

[8] S. Suthagar, T. Kumaran, G. Gowtham, T. Maridurai, T. Sathish, and S. Deivanayagi, "Computational analysis of INVELOX wind turbine to analyze the venturi velocity by change the parameter of diffuser," *Materials Today: Proceedings*, vol. 46, pp. 4245–4249, 2021.

[9] P. Kishore, P. M. Kumar, and D. Dinesh, "Wear analysis of Al 5052 alloy with varying percentage of tungsten carbide," *AIP Conf. Proc.*, vol. 2128, p. 40003, 2019.

[10] V. Govindarajan, R. Sivakumar, P. P. Patil et al., "Effect of tungsten carbide addition on the microstructure and mechanical behavior of titanium matrix developed by powder metallurgy route," *Advances in Materials Science and Engineering*, vol. 2022, Article ID 2266951, 7 pages, 2022.

[11] N. T. Hegde, D. Pai, and R. Hegde, "Heat treatment and mechanical characterisation of LM-25/tungsten carbide metal matrix composites," *Materials Today: Proceedings*, vol. 19, pp. 810–817, 2019.

[12] Y. Sesharao, T. Sathish, K. Palani et al., "Optimization on operation parameters in reinforced metal matrix of AA6066 composite with HSS and Cu," *Advances in Materials Science and Engineering*, vol. 2021, Article ID 1609769, 12 pages, 2021.

[13] F. Qiu, H. Zhang, C. L. Li et al., "Simultaneously enhanced strength and toughness of cast medium carbon steels matrix composites by trace nano-sized TiC particles," *Materials Science and Engineering A*, vol. 819, p. 141485, 2021.

[14] S. Venkatesan and M. Anthony Xavior, "Tensile behavior of aluminum alloy (AA7050) metal matrix composite reinforced with graphene fabricated by stir and squeeze cast processes," *Materials Science and Technology*, vol. 30, pp. 74–85, 2018.

[15] M. Senthilkumar, S. D. Saravanan, and S. Shankar, "Dry sliding wear and friction behavior of aluminum-rice husk ash composite using Taguchi's technique," *Journal of Composite Materials*, vol. 49, no. 18, pp. 2241–2250, 2015.

[16] N. M. Nachippan, A. Backiyaraj, V. R. Navaneeth et al., "Structural analysis of hybridized glass fiber hemp fiber reinforced composite wheel rim," *Materials Today: Proceedings*, vol. 46, pp. 3960–3965, 2021.

[17] D. Veeman, M. V. Shree, P. Sureshkumar et al., "Sustainable development of carbon nanocomposites: synthesis and classification for environmental remediation," *Journal of Nanomaterials*, vol. 2021, Article ID 5840645, 21 pages, 2021.

[18] S. Dharmalingam, R. Subramanian, and K. Somasundara Vinoth, "Analysis of dry sliding friction and wear behavior of aluminum-alumina composites using Taguchi's techniques," *Aportes de la investigación*, vol. 44, no. 18, pp. 2161–2177, 2010.

[19] P. Chenneswari, N. Sateesh, R. Subbiah, and C. Pavan, "Optimisation of machining process parameters in Al 7175 metal matrix composites using Taguchi method," *Mater. Today Proc*, vol. 46, pp. 9673–9677, 2019.

[20] M. Ramasamy, A. A. Daniel, and M. Nithya, "Investigation on surface roughness of aluminium (Al7050/TiC/BN) hybrid metal matrix," *Materials Today: Proceedings*, vol. 46, pp. 852–856, 2021.

[21] S. Kumar, T. Deepa, L. Natrayan, M. Maheedhar, and R. Kathiravan, "Evaluation of prestrain annealing impact on nanomaterial sensitization," *Journal of Nanomaterials*, vol. 2021, Article ID 3175569, 13 pages, 2021.

[22] V. Antony Vincent, C. Kailasanathan, G. Ramesh, T. Maridurai, and V. R. Arun Prakash, "Fabrication and characterization of hybrid natural fibre-reinforced sandwich composite radar wave absorbing structure for stealth radomes," *Transactions on Electrical and Electronic Materials*, vol. 22, no. 6, pp. 794–802, 2021.

[23] D. Rajesh, P. Anand, N. Lenin, V. K. Bupesh Raja, K. Palanikumar, and V. Balaji, "Investigations on the mechanical properties of tungsten carbide reinforced aluminium metal matrix composites by stir casting," *Materials Today: Proceedings*, vol. 46, pp. 3618–3620, 2021.

[24] S. Hanish Anand, N. Venkateshwaran, J. V. Sai Prasanna Kumar, D. Kumar, C. Ramesh Kumar, and T. Maridurai, "Optimization of aging, coating temperature and reinforcement ratio on biosilica toughened in-situ Al-TiB2 metal matrix composite: a Taguchi grey relational approach," *SILICON*, vol. 14, no. 8, pp. 4337–4347, 2022.

[25] L. Natrayan, S. Balaji, G. Bharathiraja, S. Kaliappan, D. Veeman, and W. D. Mammo, "Experimental investigation on mechanical properties of TiAlN thin films deposited by RF magnetron sputtering," *Journal of Nanomaterials*, vol. 2021, Article ID 5943486, 7 pages, 2021.

[26] O. P. Sharma and A. Meena, "Study of mechanical properties and wear behavior of aluminum 6061 matrix composites reinforced with hematite and titania," *Mater. Today Proc*, vol. 44, pp. 5028–5036, 2021.

[27] G. B. Veeresh Kumar, R. Pramod, C. S. P. Rao, and P. S. S. Gouda, "Artificial neural network prediction on wear of Al6061 alloy metal matrix composites reinforced with -Al_2o_3," *Materials Today: Proceedings*, vol. 5, no. 5, pp. 11268–11276, 2018.

[28] M. Sundaram, P. Prakash, S. Angalaeswari, T. Deepa, L. Natrayan, and P. Paramasivam, "Influence of process parameter on carbon nanotube field effect transistor using response surface methodology," *Journal of Nanomaterials*, vol. 2021, Article ID 7739359, 9 pages, 2021.

[29] L. Natrayan, M. Ravichandran, D. Veeman, P. Sureshkumar, T. Jagadeesha, and W. D. Mammo, "Influence of nanographite on dry sliding wear behaviour of novel encapsulated squeeze cast Al-Cu-Mg metal matrix composite using artificial neural network," *Journal of Nanomaterials*, vol. 2021, Article ID 4043196, 14 pages, 2021.

[30] C. Sri, S. Saravanamurugan, A. Shanmugasundaram, and S. Mohapatra, "Effect of SiC and Gr particles on the mechanical properties and dynamic characteristics of AA 7075 hybrid metal matrix composite," *Materials Today: Proceedings*, vol. 46, pp. 390–398, 2021.

[31] R. Pramod, G. B. Veeresh Kumar, P. S. S. Gouda, and A. T. Mathew, "A study on the Al_2O_3 reinforced Al7075 metal matrix composites wear behavior using artificial neural networks," *Materials Today: Proceedings*, vol. 5, no. 5, pp. 11376–11385, 2018.